

Synthesis of Chained-Elliptic Function Waveguide Bandpass Filter with High Rejection

Guan Shen Ng, Sovuthy Cheab, Peng Wen Wong, and Socheatra Soeung*

Abstract—This paper describes the synthesis of a bandpass filter to achieve high selectivity and rejection properties using a new class of filter functions called chained-elliptic function filters. Chained-elliptic filters have higher selectivity than Chebyshev function filters and have the property of sensitivity to manufacturing tolerance reduction in chained-function filters. The proposed design has high selectivity and reduced sensitivity, enabling easier and faster filter fabrication. The characteristic polynomials of chained-elliptic function filters are derived (through chaining elliptic filtering function) and extracted to form a coupling matrix of the bandpass filter. The novel transfer polynomials are given in detail, and a thorough investigation of the filter characteristics is performed. A theoretical comparison with Chebyshev and elliptic filters of the same order is performed to ascertain the demonstrated advantages of this proposed filter class. A high frequency narrow-band fourth-order chained-elliptic function waveguide filter centred at 28 GHz with a fractional bandwidth of 1.61% is fabricated to validate the proposed design concept. A good match among the measured, simulated, and ideal filter responses is shown where the overall responses between measurement and simulation have a difference of approximately 2% which is within the acceptable limit. The chained-elliptic function concept will be useful in designing low-cost high-performance microwave filters with various fabrication technologies for millimetre-wave applications.

1. INTRODUCTION

With the impending 5G technology, the development of high-frequency microwave filters to support the millimetre-wave spectrum has grown drastically. As the existing cellular spectra are becoming more congested, there is an urgent need of filters with sharp transition from passband to stopband for minimal spectrum wastage. For 5G implementation, the specifications for channel filters have become much more extreme and severe to accommodate more devices and users. Very high close-to-band rejections are necessary to avoid spectrum interference and at the same time optimize utilization of the allocated 5G spectrum. Theoretically, the smaller the frequency separation of return-loss (RL)/reflection zeros is, the higher the sensitivity of the filter is to any physical parameter variation [1]. Current cellular networks operate at millimeter-wave frequency range, and thus, the filter will be small in size and highly sensitive to physical parameter variation, thereby making fabrication and tuning much more difficult. In addition, narrow-band filters must be used for the 5G spectrum due to stringent channel bandwidth specifications, e.g., 50 MHz to 400 MHz channel bandwidths for frequency ranges of 24 GHz and above, where the fractional bandwidth (FBW) is less than 2%. Narrow-band filters will result in their RL zeros being scattered over an extremely narrow frequency band [1], which will further increase the sensitivity of filters to manufacturing errors, and thus, increase the fabrication time and cost. For 5G applications, the filter size will be very small (in the range of a few mm), and thus, an extremely precise

Received 20 November 2019, Accepted 11 January 2020, Scheduled 25 January 2020

* Corresponding author: Socheatra Soeung (socheatra.s@utp.edu.my).

The authors are with the Department of Electrical and Electronic Engineering, Universiti Teknologi PETRONAS, Malaysia.

fabrication process needs to be employed. Therefore, it is crucial to reduce the sensitivity of the filter to manufacturing errors to ease the fabrication and tuning processes.

Both conventional Chebyshev and elliptic filters are highly sensitive to the manufacturing tolerance, which has always been a critical issue that impedes the fabrication process, especially in waveguides, and precise computer numerical control (CNC) machining is necessary, which incurs high fabrication costs. In addition, a high sensitivity filter results in wide fluctuations of the filter response during the tuning process, and thus, a substantial amount of time will be consumed to obtain an accurate filter response. The chained-function filters introduced in [1–6] have reduced sensitivity to the manufacturing tolerance. However, the chaining process will reduce the selectivity and close-to-band rejection of the filter [1], resulting in the need for higher order filters to compensate for the reduction in selectivity and rejection properties. The reduction in selectivity and rejection properties will greatly compromise the performance of the filter, especially in narrow-band applications that require high selectivity due to the stringent spectrum utilization. Recent studies on modifying chained-function polynomials have been introduced in [7, 8], but the resulting transfer functions are all-pole functions, which limit the selectivity and close-to-band rejection improvement.

It is well established that, of all the filtering functions, the elliptic filtering function provides the best selectivity with the steepest cut-off [9–11], but this function is difficult to fabricate due to large element variations and a high sensitivity to the manufacturing tolerance. In addition, elliptic filters are canonical by nature, and thus, it is impossible to apply the group delay equalization technique in [10] to create a linear phase filter. It is possible to reduce the sensitivity to component variations in elliptic filters by reducing the Q -factor in the transfer function, resulting in a minimum Q -factor elliptic filter. However, this will deprive elliptic filters the ability to independently specify the passband and stopband ripples. Another downside of elliptic filters is that the wide out-of-band rejection is compromised. Moreover, elliptic filters have very large element value ratios [11], and thus, elliptic filters are difficult to implement using microwave technologies that have a limited range of characteristic impedances such as microstrip and coplanar waveguide filters. Therefore, most miniaturization techniques cannot be implemented using elliptic filtering functions. Elliptic filters are well-established, but unfortunately, the sensitivity of the filters to the manufacturing tolerance has not been addressed in recent studies [12–18]. In the upcoming years, the need for a filter with a low sensitivity to the manufacturing tolerance will grow drastically due to the rapid deployment of 5G communication.

In this paper, a chained-elliptic function waveguide bandpass filter is proposed to solve these problems. Sections 2 and 3 describe the formulation of chained-elliptic functions and the resulting filtering functions are tabulated. Section 4 presents a detailed theoretical exposition of chained-elliptic function characteristics, i.e., passband ripple, sensitivity to manufacturing tolerance, rejection and group delay properties. Section 5 presents the realisation procedures of the chained-elliptic function waveguide bandpass filter, reconfiguration of the filter topology and sensitivity analysis of the filter. Chained-elliptic function filters can have quasi-elliptic properties (i.e., high selectivity and close-to-band rejections) and chained-function properties (i.e., a reduced sensitivity to the manufacturing tolerance and low element values). Therefore, chained-elliptic filters are suitable for use in low-cost high frequency narrow-band applications. The filter obtained by the proposed design method is fabricated using rectangular waveguide technology, centred at 5G frequency (28 GHz) with a fractional bandwidth (FBW) of approximately 1.61% (450 MHz) to validate the proposed filter. Moreover, for the first time, a detailed theoretical exposition of chained-elliptic function properties is provided, and a comparison is made with conventional Chebyshev and elliptic approximations of the same order to verify the advantages of chained-elliptic functions.

2. CHAINED-ELLIPTIC FUNCTIONS

For the derivation of characteristic polynomials of a Butterworth approximation, the n -th order characteristic function, $K_n(\omega)$ must concentrate all its zero derivatives at the origin to produce a response that is maximally flat at the origin [10]. As a Butterworth approximation is considered an all-pole filter, all the transmission zeros are located at infinity, i.e., $P(s) = 1$, which results in poor insertion losses around cutoff, and thus, the spectrum utilization efficiency is greatly compromised. Generally, the preferred solution for elliptic approximation is when the responses of both the passband and the

stopband are equirippled, as this response gives the sharpest cutoff using Jacobian elliptic functions. Because elliptic approximation provides the steepest out-of-band rejection, the RL zeros are distributed close to each other in the passband, making the elliptic filter highly sensitive to component variations.

Butterworth polynomials are the least sensitive to component variations, as all the reflection zeros are concentrated at the origin, while elliptic polynomials have the steepest rejection and highly sensitive to component variations. Chained-elliptic functions, on the other hand, combine the advantages of the Butterworth and elliptic approximations to solve the problems of high sensitivity, high loss, and low rejection properties. In chained-elliptic functions, a compromise can be made between low sensitivity, low resonator unloaded- Q , and the low loss filter properties of Butterworth filters with the high close-to-band rejection of elliptic filters. With the chained-elliptic function, a new polynomial generating function can be defined by the product of μ functions, called seed-functions, each with a different prescribed multiplicity $m_{(s(k))}$ [2], resulting in the possibility of different combinations of seed-function orders to produce different transfer functions of the same order.

The number of possible seed-function combinations $SFC(n_T)$ is in the following form [1, 4, 20]:

$$SFC(n_T) \equiv P(n_T), \tag{1}$$

where $P(n_T)$ is the partition function, which provides a number of unrestricted decompositions of an integer number (n_T) as a sum of smaller integers, without regards to the order. For instance, if $n_T = 4$, there are five possible combinations because $P(4) = 5$ as:

$$\begin{aligned} &4 \\ &1 + 3 \\ &2 + 2 \\ &1 + 1 + 2 \\ &1 + 1 + 1 + 1 \end{aligned}$$

Therefore, a fourth-order chained-elliptic function filter can be formulated by a second-order seed function with a multiplicity of two (i.e., a squared second-order seed function) or by chaining a third-order chained-elliptic function with a first-order seed function, both having a multiplicity of one. The resulting seed functions will always have an elliptic and Butterworth polynomial of order n_T . Because a symmetrical odd-order elliptic function will always have at least one pole at the origin, chaining a symmetrical odd-order elliptic polynomial with only a Butterworth polynomial of any multiplicity will not result in an increment of the RL zeros frequency separation, as the number of poles will always be the same. This concept also applies to powered seed functions (e.g., a squared third order or a cubed third order). Furthermore, chained-elliptic functions can result in quasi-elliptic responses.

3. POLYNOMIAL GENERATION

The formulation of chained-elliptic functions follows the same transfer function approximation for classical filters [5–7]. The general representation of the squared magnitude response is in the following form:

$$|S_{21}(j\omega)|^2 = \frac{1}{1 + \epsilon^2 K_{n_T}(\omega)^2}, \tag{2}$$

where ϵ = the ripple factor, which controls passband ripple, and $K_n(\omega)$ is the filtering function of degree n_T . The filtering function can be defined as $K_n(\omega) \equiv G_\mu(\omega)$, where $G_\mu(\omega)$ is the product of μ seed functions $S_{(n_{(s(k))})}(\omega)$ as [1, 20]

$$G_\mu(\omega) = \prod_{k=1}^{\mu} (S_{n_{s(k)}}(\omega))^{m_{s(k)}}, \tag{3}$$

where $n_{(s(k))}$ is the k th seed function order with multiplicity $m_{(s(k))}$. The degree n_T is formed by the summation of constituent functions as [1, 20]

$$n_T = \sum_{k=1}^{\mu} n_{s(k)} m_{s(k)}. \tag{4}$$

Elliptic functions can be used as the seed function, and thus, seed functions can be defined as [19]

$$S_{n_s(k)}(\omega) = \prod_{i=1}^{\frac{n_s(k)}{2}} \frac{\omega_i^2 - \omega^2}{1 - \omega_i^2 \omega^2}, \quad \text{for } n_s(k) = \text{even} \quad (5a)$$

and

$$S_{n_s(k)}(\omega) = \prod_{i=1}^{\frac{n_s(k)}{2}} \frac{\omega_i^2 - \omega^2}{1 - \omega_i^2 \omega^2}, \quad \text{for } n_s(k) = \text{odd} \quad (5b)$$

where ω_i is the position of the i -th transmission zero. Once n_T is defined, the formulation of all possible seed functions follows the steps in [1]. Once all the seed functions are evaluated, the chained-elliptic characteristic functions $G_\mu(\omega)$ can be finalized. Tables 1–3 show the chained-elliptic characteristic functions for $n_T = 4, 5$, and 6 , respectively, formed by elliptic seed functions. The first row in each table corresponds to a Butterworth polynomial, while the last row in each table corresponds to an elliptic polynomial of order n_T . The equations used to formulate the elliptic polynomials can be found in the literature [19].

Table 1. Chained-elliptic filtering functions for $n_T = 4$.

No. of Seed Functions	Orders of the Seed Functions	Chained-Elliptic Filtering Functions
4	1, 1, 1, 1	ω^4
3	1, 1, 2	$-\frac{32.671(\omega^4 - 0.101\omega^2)}{\omega^2 - 9.899}$
2	2, 2	$\frac{1067.390(\omega^2 - 0.101)^2}{(\omega^2 - 9.899)^2}$
2	1, 3	$\frac{8.747j(\omega^4 - 0.388\omega^2)}{\omega^2 - 2.577}$
1	4	$\frac{118.511(\omega^4 - 0.619\omega^2 + 0.053)}{\omega^4 - 11.680\omega^2 + 18.855}$

Table 2. Chained-elliptic filtering functions for $n_T = 5$.

No. of Seed Functions	Orders of the Seed Functions	Chained-Elliptic Filtering Functions
5	1, 1, 1, 1, 1	ω^5
4	1, 1, 1, 2	$-\frac{32.671(\omega^5 - 0.101\omega^3)}{\omega^2 - 9.899}$
3	1, 2, 2	$\frac{1067.390(\omega^3 - 0.101\omega)^2}{(\omega^2 - 9.899)^2}$
3	1, 1, 3	$\frac{8.747j(\omega^5 - 0.388\omega^3)}{\omega^2 - 2.577}$
2	1, 4	$\frac{118.511(\omega^5 - 0.620\omega^3 + 0.053\omega)}{\omega^4 - 11.680\omega^2 + 18.855}$
2	2, 3	$-\frac{285.764j(\omega^3 - 0.388\omega)(\omega^2 - 0.101)}{(\omega^2 - 2.577)(\omega^2 - 9.899)}$
1	5	$\frac{40.005j(\omega^5 - 0.972\omega^3 + 0.204\omega)}{\omega^4 - 4.767\omega^2 + 4.905}$

For the elliptic formulations of different orders, the passband frequency, ω_p , and the maximum passband loss, A_p , are kept constant. Therefore, the resulting elliptic functions will have the same RL level (RL = -10 dB) and passband frequency ($\omega_p = 1$) regardless of the order, N . The stopband frequency, ω_s , and the minimum stopband loss, A_s , are changed accordingly to result in different orders, N , ranging from two to six. By predefining the elliptic functions of order two to six, chaining can be

Table 3. Chained-elliptic filtering functions for $n_T = 6$.

No. of Seed Functions	Orders of the Seed Functions	Chained-Elliptic Filtering Functions
6	1, 1, 1, 1, 1, 1	ω^6
5	1, 1, 1, 1, 2	$-\frac{32.671(\omega^6-0.101\omega^4)}{\omega^2-9.899}$
4	1, 1, 2, 2	$\frac{1067.390(\omega^4-0.101\omega^2)^2}{(\omega^2-9.899)^2}$
4	1, 1, 1, 3	$\frac{8.747j(\omega^6-0.388\omega^4)}{\omega^2-2.577}$
3	1, 2, 3	$-\frac{285.764j\omega(\omega^3-0.388\omega)(\omega^2-0.101)}{(\omega^2-2.577)(\omega^2-9.899)}$
3	1, 1, 4	$\frac{118.511(\omega^6-0.620\omega^4+0.053\omega^2)}{\omega^4-11.680\omega^2+18.855}$
3	2, 2, 2	$-\frac{34872.517(\omega^2-0.101)^3}{(\omega^2-9.899)^3}$
2	3, 3	$-\frac{76.505(\omega^3-0.388\omega)^2}{(\omega^2-2.577)^2}$
2	2, 4	$\frac{3871.870(\omega^4-0.620\omega^2+0.053)(\omega^2-0.101)}{(\omega^4-11.680\omega^2+18.855)(\omega^2-9.899)}$
2	1, 5	$\frac{40.005j(\omega^6-0.972\omega^4+0.204\omega^2)}{\omega^4-4.767\omega^2-4.905}$
1	6	$\frac{209.293(\omega^6-1.432\omega^4+0.555\omega^2-0.04)}{\omega^6-13.903\omega^4+35.882\omega^2-25.057}$

performed accordingly to form the chained-elliptic filtering functions, as shown in Tables 1–3. In the next section, an in-depth analysis is carried out to explore the characteristics of the resulting polynomials.

4. CHARACTERISTICS OF CHAINED-ELLIPTIC FUNCTION FILTERS

In microwave filters, there are several key characteristics that must be carefully defined to produce a high-performance filter. The most crucial characteristics to define the performance of a filter are insertion and return losses and group-delay responses. Generally, emphasis should be placed on analysing the steady-state frequency-domain responses and transient time-domain responses to ensure the overall performance of the filter. These responses are identified from the characteristic polynomials in a normalised low-pass prototype and can be transformed easily to desired high-pass, bandpass, or bandstop designs using suitable transformation methods. For simplicity, a normalised low-pass prototype is used for the exposition of chained-elliptic function filters.

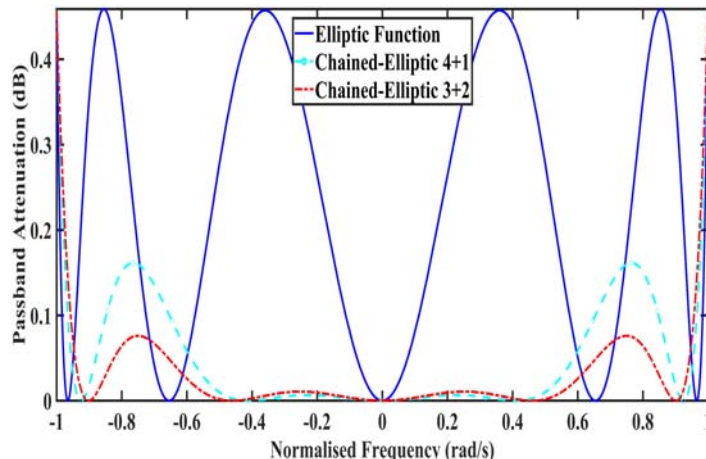


Figure 1. Passband attenuation of fifth-order elliptic and chained-elliptic functions.

4.1. Chained-Elliptic Function Filters Passband Ripple

A chained-elliptic approximation has better close-to-band rejection than Butterworth and Chebyshev approximations, but its rejection is slightly inferior compared to an elliptic approximation, as the chaining procedure will disrupt the optimum properties of the elliptic function. Therefore, both the stopband rejection and passband equiripple properties will be affected. Fig. 1 shows the passband ripple for a fifth-order chained-elliptic filter with elliptic approximation (RL = -10 dB). From Fig. 1, chained-elliptic functions will result in a lower ripple level compared to elliptic functions while distorting the equiripple properties of the elliptic. A quasi-equiripple response is possible by selecting a powered seed function [1]. In addition, chaining odd-order elliptic function with a Butterworth approximation will also result in a quasi-elliptic response, as shown in Fig. 2 (i.e., chained-elliptic function (5 + 1)).

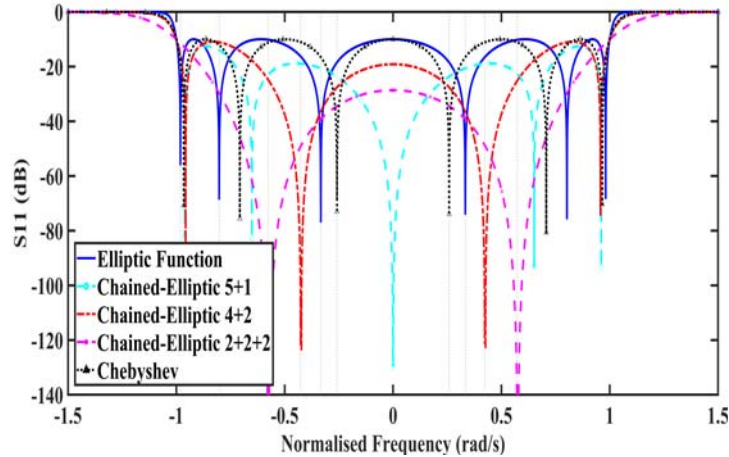


Figure 2. Return loss of sixth-order elliptic, chained-elliptic and Chebyshev functions.

4.2. Placement of Reflection Zeros in Chained-Elliptic Function Filters

Figure 2 shows the placement of reflection zeros of elliptic and conventional Chebyshev filters (RL = -10 dB) with chained-elliptic function filters. The RL level of the chained-elliptic function filter will not exceed the predefined level for all seed-function combinations, as shown in Fig. 2. It must be noted that the chained-elliptic (4 + 2) has six reflection zeros with two pairs ($\omega \sim 0.4$) closely positioned to each other. Theoretically, the relative frequency separation of reflection zeros will affect the sensitivity of the filter to physical variations, which is a crucial factor in achieving tuning-less implementation. The reflection zeros are not equally spaced in the passband, and the zeros with the nearest proximity to the cutoff frequency will have the smallest gap in frequency separation. The relative frequency separation between the nearest spaced zeros can be approximated as [1]

$$\delta\omega_{\min} = 2 \sin\left(\frac{\pi}{n_{s(k)}}\right) \sin\left(\frac{\pi}{2n_{s(k)}}\right) \quad (6)$$

As the filter order increases, the minimum frequency separation of reflection zeros decreases. From Eq. (6), it is found that the maximum frequency separation of reflection zeros can be acquired from a second-order seed function. However, using a second-order seed function will result in lower out-of-band rejection. One of the key advantages of the chained-elliptic is that it allows designers to use powered seed functions to achieve the desired rejection while at the same time maintaining the sensitivity obtained from the predefined seed function. In addition, this concept also applies to chaining an odd-order seed function with only a Butterworth function of any multiplicity or powered odd-order seed functions with Butterworth functions. This odd-order chaining method is extremely useful to reduce the sensitivity of odd-order chained-elliptic functions, as the sensitivity to manufacturing tolerance can be maintained even when the order increases. These methods effectively place multiple reflection zeros at the same

frequencies, and thus, both odd and even-order chained-elliptic functions can have a sensitivity reduction using the above methods.

4.3. Rejection Characteristics of Chained-Elliptic Function Filters

As previously mentioned, the selectivity of chained-elliptic filters is better than that of conventional Chebyshev filters but worse than that of elliptic filters of the same order. It is universally recognised that elliptic filters have the sharpest cutoff among all known filter classes [10], which means that they are unrivalled in producing the best close-to-band rejection. However, they are seldom employed in real-life applications because elliptic filters are highly sensitive to component variations, and thus, high-end (extremely precise) manufacturing processes must be employed. Further, elliptic filters have large element value ratios, making them difficult to implement in other technologies that have a limited range of characteristic impedances. Although elliptic filters have the best selectivity, all the disadvantages make their fabrication very challenging. Therefore, conventional Chebyshev filters are used instead due to their simplicity and passable rejection properties.

Figure 3(a) shows the transfer responses for fourth-order elliptic (RL = -10 dB), Chebyshev (RL = -17.5 dB) and chained-elliptic functions. The RL level of the Chebyshev function is purposely tuned to match the RL level in the chained-elliptic function with a third-order and first-order (3 + 1) combination. It is evident that chained-elliptic functions have better close-to-band rejection than Chebyshev approximations (with the same ripple level) but worse rejection than elliptic approximations. Therefore, a chained-elliptic function of any seed-function combination will always have a high selectivity and at least one pair of transmission zeros (TZ), which is very important in narrow-band applications for which the spectrum utilization is extremely stringent. As mentioned previously, chained-elliptic functions can have a reduced sensitivity, and thus, the fabrication hurdle (i.e., the sensitivity to component variations) in producing a quasi-elliptic response can be solved easily. With chained-elliptic function filters, users can meet the required close-to-band rejection with reduced sensitivity, making the realisation of a high selectivity filter much simpler.

Figure 3(b) shows the transfer response of a sixth-order chained-elliptic with both sixth-order elliptic and conventional Chebyshev (RL = -10 dB) approximations. The RL level of the Chebyshev approximation is made to be the same as that of the elliptic, and it is evident that the chained-elliptic rejections become much better at higher orders even though it can be improved further by predefining a better selectivity during the elliptic formulation stage. The number of TZs in the chained-elliptic is dependent on the resulting position of the TZs in the elliptic approximations. For example, if two

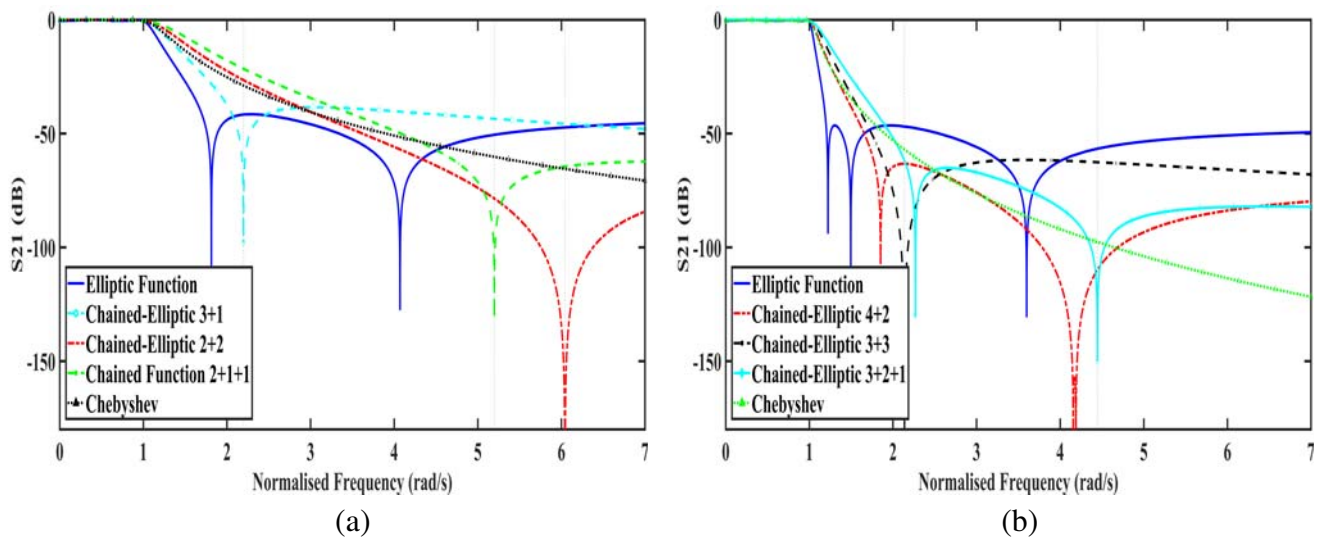


Figure 3. Transfer responses: (a) fourth-order elliptic, chained-elliptic and Chebyshev functions and (b) sixth-order elliptic, chained-elliptic and Chebyshev functions.

third-order seed function has the same TZ position, the resulting TZ will be the same, resulting in better stopband rejection, as shown in Fig. 3(b). Because powered seed functions will have multiple TZs at the same frequencies, the stopband rejection level can be improved. From Fig. 3(b), it is apparent that chained-elliptic functions have better stopband attenuation than elliptic functions.

Elliptic filters have an excellent close-to-band rejection. However, they have a poor wide out-of-band rejection. This is because elliptic filters will have all TZs concentrated at finite frequencies to produce a high selectivity, thus limiting the wide out-of-band rejection. Limiting the wide out-of-band rejection will have a major impact on other signals, as elliptic filters might interfere with other signals of different frequency bands. In the chained-elliptic function, this can be solved by chaining the elliptic seed function with the Butterworth seed function, which will result in decaying out-of-band rejection, as seen in Fig. 3. This is because the Butterworth function will always have a TZ at infinity, and thus, the rejection slope will slowly decay to negative infinity (dB). The chained-elliptic can bridge between the high close-to-band rejection of the elliptic without compromising the wide out-of-band rejection properties of Butterworth approximations. Therefore, chained-elliptic filters reduce the possibility of interfering with other signals of different spectrums.

4.4. Group Delay Properties of Chained-Elliptic Function Filters

Group delay is crucial in measuring signal distortion due to phase differences for different frequencies. Therefore, group delay can be computed by finding the derivative of the phase with respect to angular frequency. Group delay also can reveal a filter's loss characteristics, and as the selectivity of the filter increases, the group-delay distortion near the cutoff frequency becomes sharper, which will result in a longer delay for signals with frequencies near the cutoff, and thus, result in more attenuation [1]. Fig. 4 shows the group delay responses of sixth-order elliptic and Chebyshev (RL = -10 dB) approximations with various sixth-order chained-elliptic functions. From Fig. 4, the chained-elliptic (5 + 1) function is more selective than the Chebyshev approximation, and as mentioned previously, chained-elliptic functions usually have a higher selectivity than Chebyshev functions in the same ripple level (mostly for quasi-equiripple functions). As seen in Fig. 4, chained-elliptic functions can have lower passband edge deviations compared to Chebyshev approximations, but the selectivity will be compromised. However, this will also result in a smaller implementation loss. By selecting chained-elliptic filters that have lower group delays than conventional Chebyshev filters, the passband frequencies will suffer less attenuation from losses, as they remain within the filter for a shorter time. Different seed-functions combinations will result in different group delay properties.

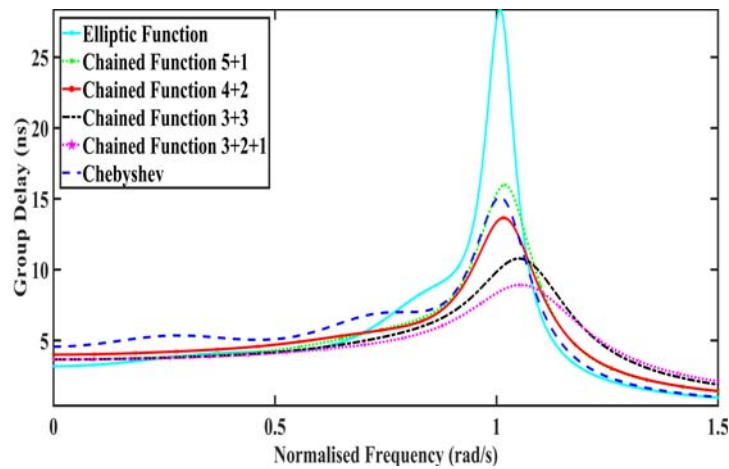


Figure 4. Group-delay responses for sixth-order elliptic, Chebyshev and chained-elliptic functions.

5. CHAINED-ELLIPTIC FUNCTION FILTER REALISATION

For the realisation of a prototype, a fourth-order chained-elliptic filter with a third- and first-order seed function combination (i.e., 3 + 1) is selected. This combination is selected because it has the best overall rejection properties among all the seed-function combinations in a fourth-order chained-elliptic function. As mentioned in Section 4, chaining an odd-order seed function with a Butterworth function (TZ at infinity) will result in a slowly decaying out-of-band rejection without affecting the sensitivity, and thus, the filter will have TZs at both finite and infinite frequencies. Therefore, the filter will have high close-to-band rejection without compromising the far out-of-band rejection. The transfer polynomial for this filter is given in Table 1.

5.1. Topology of Chained-Elliptic Function Filters

Once the characteristic polynomials of the chained-elliptic function (3 + 1) are acquired from the transfer polynomial in Table 1, a double-terminated coupling matrix (N + 2) can be derived as in [10, 21, 22]. The initial form of the coupling matrix has many unwanted couplings in its entries which are physically impossible to be realised and similarity transformations (rotations) are performed to eliminate these couplings following the procedures in [10]. The final N + 2 coupling matrix after similarity transformations is

$$M = \begin{bmatrix} 0 & 1.0533 & 0 & 0 & 0 & 0 \\ 1.0533 & 0 & 0.8654 & 0 & -0.1118 & 0 \\ 0 & 0.8654 & 0 & 0.7506 & 0 & 0 \\ 0 & 0 & 0.7506 & 0 & 0.8654 & 0 \\ 0 & -0.1118 & 0 & 0.8654 & 0 & 1.0533 \\ 0 & 0 & 0 & 0 & 1.0533 & 0 \end{bmatrix} \tag{7}$$

Based on Eq. (7), the topology of the prototype can be synthesised, as in Fig. 5 where the resonator is represented by solid circles, and the source/load is represented by hollow circles. A cross coupling between resonator 1 and resonator 4 is expected to allow the realization of TZ in chained-elliptic function (3 + 1) for high close-to-band rejection. The frequency is shifted using method in [11] where ω is substituted as:

$$\omega \rightarrow \alpha \frac{\lambda_g}{\lambda_{g0}} \sin \left(\pi \frac{\lambda_{g0}}{\lambda_g} \right), \tag{8a}$$

and

$$\lambda_g = \frac{c}{f \times \sqrt{1 - \frac{f_c^2}{f^2}}}, \tag{8b}$$

$$\lambda_{g0} = \frac{\lambda_{g1} + \lambda_{g2}}{2} \tag{8c}$$

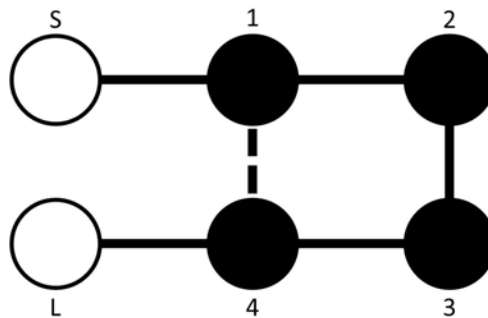


Figure 5. Filter topology (the solid line represents main-line coupling, and the dotted line represents cross-coupling).

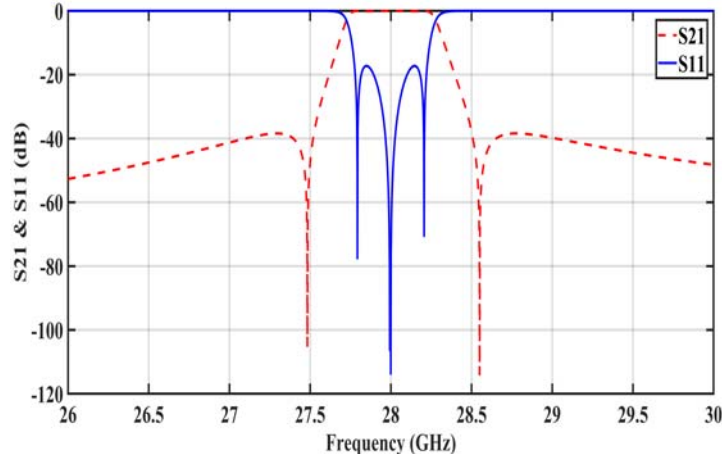


Figure 6. Theoretical transfer and reflection responses of chained-elliptic function (3 + 1) filter.

$$\alpha = \left(\frac{\lambda_{g1}}{\lambda_{g0}} \sin \frac{\pi \times \lambda_{g0}}{\lambda_{g1}} \right)^{-1} \quad (8d)$$

where α is the attenuation constant, λ_g the guide wavelength, and λ_{g0} the guide waveguide wavelength when the guide is half-wavelength long; λ_{g1} and λ_{g2} are guide-wavelengths at band-edge frequencies; f is frequency (Hz); f_c is cutoff frequency ($= 17.357$ GHz); and c is speed of light (3×10^8 m/s).

Figure 6 shows the theoretical transfer and reflection responses after frequency shifting. The subsequent step will be converting the coupling matrix in Eq. (7) into waveguide physical dimensions. The resonator length can be estimated using [10], where:

$$\begin{aligned} \theta_{1j} &= \frac{n\pi}{2} + \frac{1}{2} \left(\cot^{-1} \frac{B_{ij}}{2} - \sin^{-1}(B_{jl} - B_{jj}) \right) \\ \theta_{2j} &= \frac{n\pi}{2} + \frac{1}{2} \left(\cot^{-1} \frac{B_{jk}}{2} - \sin^{-1}(B_{jl} - B_{jj}) \right) \end{aligned} \quad (9)$$

where $\theta_{1j} + \theta_{2i} \equiv$ the total electrical length in radian; n is the number of half-wavelengths; B_{ij} and B_{jk} are the end-wall susceptance; B_{jl} is the sidewall coupling; and B_{ij} is the offset factor. The cutoff frequency of the waveguide in TE-mode is [24]:

$$f_{mnp} = \frac{c}{2\pi\sqrt{\mu_r\epsilon_r}} \sqrt{\left(\frac{m\pi}{a}\right)^2 + \left(\frac{n\pi}{b}\right)^2 + \left(\frac{p\pi}{d}\right)^2} \quad (10)$$

where m , n , and p are numbers of half-wavelength variations in the standing wave pattern in x , y , z directions, respectively; μ_r and ϵ_r are the permeability and permittivity of the material inside the cavity. Using Eq. (10), the width, a , and height, b , can be computed to find the dimension of the waveguide cavity. Since the dominant mode of rectangular waveguide is TE₁₀, the height, b , will be half of the width, a . Filters with cross-couplings should be implemented in folded topology, and the design techniques to realize filters with folded topology (cross-couplings) can be found in [23–26].

5.2. Chained-Elliptic Function Filters Prototype Design

The filter topology is implemented in a fourth-order single bandpass WR-34 (8.636 mm \times 4.318 mm) waveguide filter with a cutoff of 17.357 GHz, as shown in Fig. 7, using the Ansys HFSS simulation software. Since the design is in folded topology, waveguide flange cannot be attached, and thus, SMA (Sub-Miniature version A) connectors are attached for measurement. The filter is designed to have a return loss of 17.3 dB, with a centred frequency of 28 GHz for high-frequency applications, and a fractional bandwidth of 1.61% (BW = 450 MHz) to depict a narrow-band filter. All physical dimensions of the fourth-order chained-elliptic waveguide filter are shown in Table 4. Inductive irises are used for

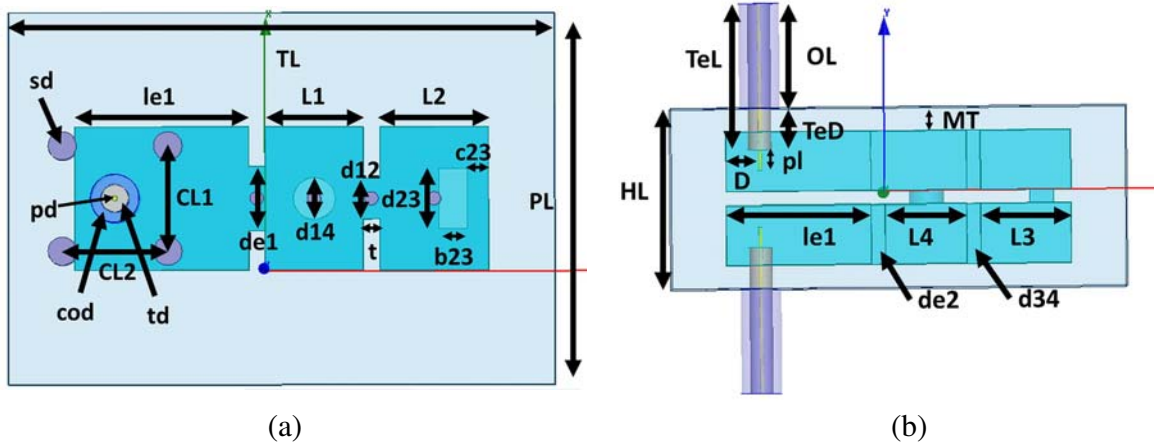


Figure 7. Fourth-order chained-elliptic function waveguide filter: (a) top view and (b) side view.

Table 4. Fourth-order chained-elliptic function (3 + 1) bandpass waveguide filter dimensions.

Symbol	Dimension (mm)	Symbol	Dimension (mm)	Symbol	Dimension (mm)
$L1$	5.9	TL	32.87	$d12$	2.45
$L2$	6.52	PL	22.4	$d23$	3.64
$L3$	6.52	HL	13.04	$d34$	2.45
$L4$	5.9	MT	1.7	$d14$	2.51
t	1	OL	7.6	$b23$	1.71
$de1$	3.88	TeD	3	$c23$	1.25
$de2$	3.88	TeL	10.6	cod	2.92
td	1.67	pd	0.3	pl	1.5

the inline resonator couplings while resonant irises are used for folded resonator couplings. There will be a cross coupling between the first resonator and the last resonator due to the presence of a pair of TZs, and a cylindrical iris is used to induce the cross coupling as shown in Fig. 7(b). The circular resonant iris (cross coupling) between first and last resonators will affect the position of the TZs. Increasing the dimension of the circular resonant iris opening (stronger capacitive coupling) will result in higher selectivity while lowering the stopband rejection.

Figure 8 shows the fabricated filter with tuning screws and SMA connectors attached to it. The SMA connectors have a diameter of 2.92 mm, and the walls of the waveguide are made from aluminium. Measurement of the filter are done using Agilent E8363C PNA network analyzer and 85056d calibration kit are used for calibration. Fig. 9 shows the transfer and reflection responses of the simulated and measured results of a fourth-order chained-elliptic function waveguide filter.

For the simulated result, the insertion loss is less than -1 dB, and the return loss is -15.5 dB, while the measured prototype has an insertion loss less than -1.6 dB and a return loss of -11.35 dB. The resonant frequency of simulated response is 27.975 GHz while the resonant frequency of measured response is 28.085 GHz which results in a shift of 0.39% in resonant frequency. In addition, the bandwidth percentage difference between simulated (510 MHz) and measured (480 MHz) is 5.88%. The TZs for simulated are at 27.38 GHz and 28.63 GHz while the measured TZs are at 27.6 GHz and 28.6 GHz. For 30 dB rejection, the higher frequency is shifted by 0.07% while the lower frequency is shifted by 0.65%. The frequency shifting of the measured response is within the acceptable limit of $\pm 1\%$ tolerance error in Fig. 11. Since lossless condition is not possible, i.e., the conductivity of aluminium cannot be infinity, the fabricated filter have higher insertion loss and lower return loss as compared to the simulated

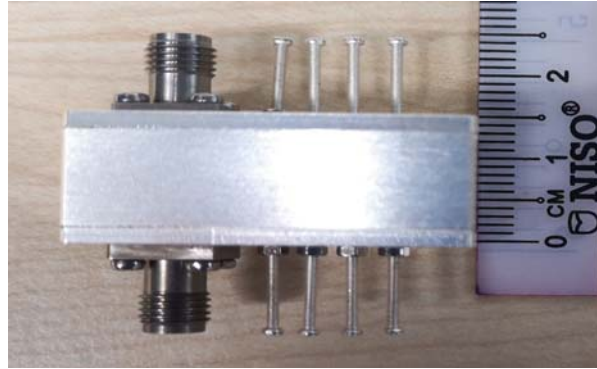


Figure 8. Fabricated fourth-order chained-elliptic function waveguide filter.

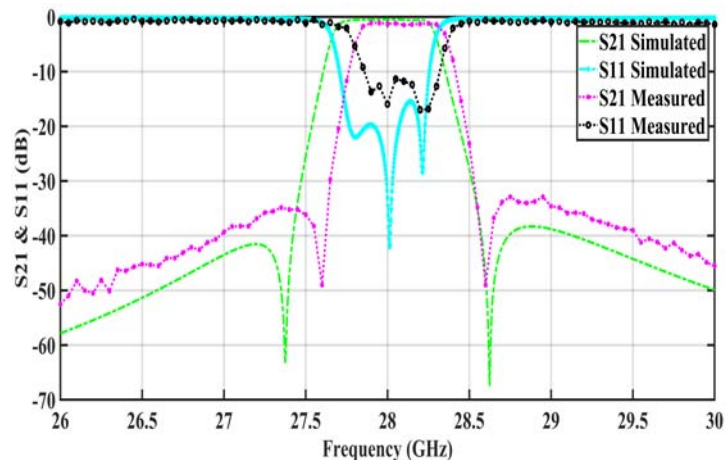


Figure 9. Transfer and reflection responses of simulated and measured fourth-order chained-elliptic function waveguide filter.

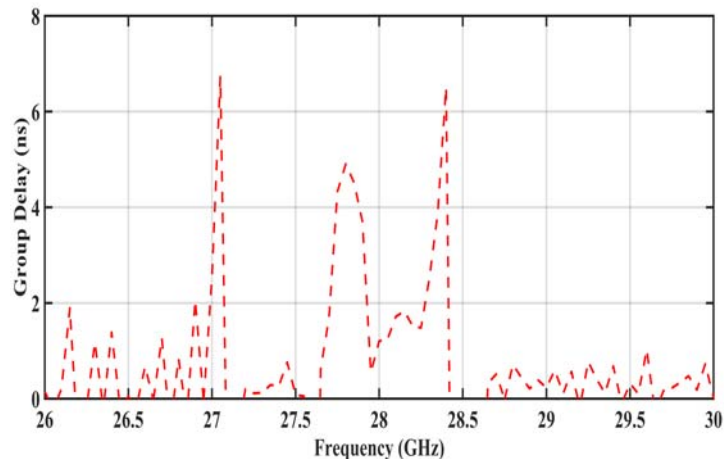


Figure 10. Chained-elliptic function waveguide filter group delay.

filter. The resonators and irises are not perfectly rectangle due to limitation of CNC machining process which resulting in slight curving at the edges. This results in shrinkage of the bandwidth and the responses shifted to the right. As the CNC machining have a ± 0.05 mm manufacturing tolerance, the fabricated responses slight deviation is acceptable. Minimal tuning is performed to achieve the required

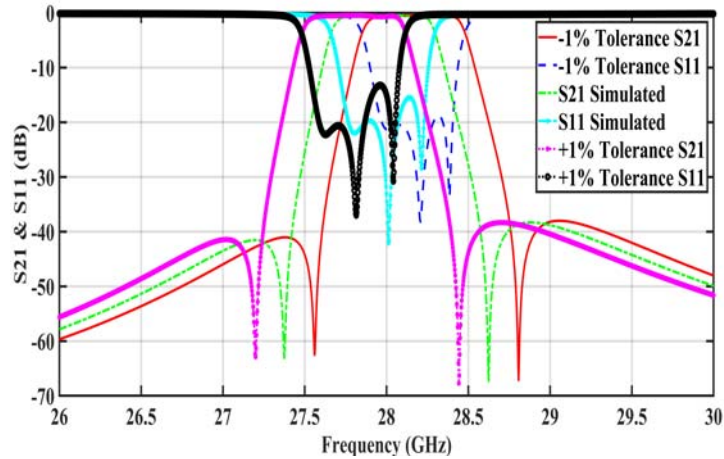


Figure 11. Simulated S_{21} and S_{11} responses with tolerance $\pm 1\%$.

transfer and reflection responses. Fig. 10 shows the group delay of the fabricated chained-elliptic filter. It is apparent that the filter is highly selective, as there is a sharp group delay distortion near the cutoff frequencies.

Table 5 shows the properties of the chained-elliptic, Chebyshev, and elliptic filters. The element value ratio, $\frac{g_{max}}{g_{min}}$, of the chained-elliptic filter is much lower than that of the elliptic filter but slightly higher than that of the Chebyshev filter. However, different seed-function combinations will offer different $\frac{g_{max}}{g_{min}}$ ratios; some are larger, and some are smaller than those of the Chebyshev filter. Therefore, the chained-elliptic (3 + 1) filter can be implemented using other technologies that have a limited range of characteristic impedances. The element value ratio is a crucial parameter in filter design, as smaller element value ratios allow more implementation technologies, especially in filter miniaturisation wherein the range of characteristic impedances is greatly limited. In addition, the chained-elliptic (3 + 1) filter will result in lower RL levels than the elliptic filter and have better selectivity than the Chebyshev filter in the same ripple level. The chained-elliptic (3 + 1) filter also provides better wide out-of-band rejection than the elliptic filter, which will slowly decay, as there is a TZ at infinity (the TZ from the Butterworth function), but worse rejection than the Chebyshev filter. Chebyshev filters generally need a higher order than chained-elliptic filters to have comparable performances.

Table 5. Properties of Chebyshev, elliptic and chained-elliptic function filters.

Filter Class	Order (N)	Return Loss (dB)	$\frac{g_{max}}{g_{min}}$	Stopband at $\omega = 7$ (dB)
Chebyshev	5	20	1.761	-88
Elliptic	4	10	52	-45
Chained-elliptic (3 + 1)	4	17.3	8.92	-50

5.3. Sensitivity of Chained-Elliptic Function Filters

As mentioned previously, the chained-elliptic filter can result in sensitivity reduction, which means that the chained-elliptic filter is less affected by component variations. For a quick analysis of the sensitivity of the proposed filter, the physical dimensions of the resonators and irises in Table 4 are altered by $\pm 1\%$ to estimate the sensitivity of the filter and the transfer and reflection responses are shown in Fig. 11. It is apparent that the chained-elliptic (3 + 1) filter is less sensitive to physical variations, as the responses are not greatly affected even after a tolerance of $\pm 1\%$ is applied, as shown in Fig. 11. The number of transfer zeros and poles remains the same after the tolerance is applied. The insertion loss and stopband attenuation are not affected much after the tolerance. However, the transfer and reflection responses

are slightly shifted to the left when a +1% tolerance is applied and slightly shifted to the right when a -1% tolerance is applied. This is because the resonator lengths are varied, and larger resonator lengths result in lower frequency shifts (i.e., responses shifted to the left), while smaller resonator lengths result in higher frequency shifts (i.e., responses shifted to the right).

6. CONCLUSION

Chained-elliptic function filters offer a variety of transfer functions, and each transfer function provides different filter and implementation characteristics. Chained-elliptic function filters with different seed-function combinations will have different implementation characteristics and can be used to extend state-of-the-art filters toward higher frequencies or narrower frequency bands or to lower the accuracy, fabrication costs and tuning time for a given set of filter specifications. Chained-elliptic filters can provide quasi-elliptic and quasi-equiripple responses without compromising the wide out-of-band rejection. In addition, chained-elliptic filters can be implemented with different implementation technologies, even those with a limited range of characteristic impedances. Chained-elliptic function filters provide a compromise between the low sensitivity of the Butterworth filter and the high close-to-band rejection properties of the elliptic filter. Sensitivity reduction can be achieved by selecting powered seed-functions or by chaining odd-order seed functions with Butterworth filters of any multiplicity. With the reduction in sensitivity to the manufacturing tolerance, chained-elliptic function filters allow low-cost fabrication and a faster tuning process. This technique will be useful in designing high frequency narrow-band filters. Therefore, chained-elliptic filters are an alluring alternative solution to low cost, high-performance microwave and millimetre-wave bandpass filters.

ACKNOWLEDGMENT

The authors would like to thank Universiti Teknologi PETRONAS for YUTP (015LC0-093) funding and Ministry of Higher Education Malaysia for PRGS (0153AB-L50) funding on the research as well as FILPAL for the support.

REFERENCES

1. Chrisostomidis, C. E. and S. Lucyszyn, "On the theory of chained-function filters," *IEEE Transactions on Microwave Theory and Techniques*, Vol. 53, No. 10, 3142–3151, Oct. 2005.
2. Guglielmi, M. and G. Connor, "Chained function filters," *IEEE Microw. Guided Wave Lett.*, Vol. 7, No. 12, 390–392, Dec. 1997.
3. Chrisostomidis, C. E. and S. Lucyszyn, "Seed function combination selection for chained function filters," *IET Microwaves, Antennas and Propagation*, Vol. 4, 799–807, Jun. 2010.
4. Chrisostomidis, C. E., M. Guglielmi, P. Young, and S. Lucyszyn, "Application of chained functions to low-cost microwave band-pass filters using standard PCB etching techniques," *2000 30th European Microwave Conference*, Oct. 2000.
5. Lim, Y. P., Y. L. Toh, S. Cheab, G. S. Ng, and P. W. Wong, "Chained-function waveguide filter for 5G and beyond," *TENCON 2018 — 2018 IEEE Region 10 Conference*, 2018.
6. Lim, Y. P., Y. L. Toh, S. Cheab, S. Lucyszyn, and P. W. Wong, "Coupling matrix synthesis and design of a chained-function waveguide filter," *2018 Asia-Pacific Microwave Conference (APMC)*, 2018.
7. Perenic, G., N. Stamenkovic, N. Stojanovic, and N. Denic, "Chained-function filter synthesis based on the modified Jacobi polynomials," *Radioengineering*, Vol. 27, No. 4, 1112–1118, 2018.
8. Stojanović, N., N. Stamenković, and I. Krstić, "Chained-function filter synthesis based on the Legendre polynomials," *Circuits, Systems, and Signal Processing*, Vol. 37, No. 5, 2001–2020, Aug. 2017.

9. Zverev, A. I., *Handbook of Filter Synthesis*, Wiley, New York, 1967.
10. Cameron, R. J., C. M. Kudsia, and R. R. Mansour, *Microwave Filters for Communication Systems: Fundamentals, Design, and Applications*, 2nd Edition, Wiley, New York, Apr. 2018.
11. Hunter, I., *Theory and Design of Microwave Filters*, (IET Electromagnetic Waves Series), 370, The Institution of Engineering and Technology, London, United Kingdom, 2006.
12. Xu, J., "Compact quasi-elliptic response wideband bandpass filter with four transmission zeros," *IEEE Microwave and Wireless Components Letters*, Vol. 25, No. 3, 169–171, 2015.
13. Chen, S., L.-F. Shi, G.-X. Liu, and J.-H. Xun, "An alternate circuit for narrow-bandpass elliptic microstrip filter design," *IEEE Microwave and Wireless Components Letters*, Vol. 27, No. 7, 624–626, 2017.
14. Chen, C.-J., "A coupled-line coupling structure for the design of quasi-elliptic bandpass filters," *IEEE Transactions on Microwave Theory and Techniques*, Vol. 66, No. 4, 1921–1925, 2018.
15. Zhang, F., J. Li, P. Zhao, G. Huang, and J. Xu, "A wideband microstrip elliptic bandpass filter with flexibly tunable bandwidth," *2018 International Conference on Microwave and Millimeter Wave Technology (ICMMT)*, 2018.
16. Dimopoulos, H. G., "Optimal use of some classical approximations in filter design," *IEEE Transactions on Circuits and Systems II: Express Briefs*, Vol. 54, No. 9, 780–784, 2007.
17. Wang, L. and L. Jin, "A quasi-elliptic microstrip bandpass filter using modified anti-parallel coupled-line," *Progress In Electromagnetics Research*, Vol. 138, 245–253, 2013.
18. Kuo, J.-T., S.-C. Tang, and S.-H. Lin, "Quasi-elliptic function bandpass filter with upper stopband extension and high rejection level using cross-coupled stepped-impedance resonators," *Progress In Electromagnetics Research*, Vol. 114, 395–405, 2011.
19. Poularikas, A., *The Handbook of Formulas and Tables for Signal Processing*, CRC Press, Boca Raton, Fla., 1999.
20. Chisostomidis, C. E., "Chained function filters — Theory and applications," Ph.D. dissertation, Univ. Surrey, Surrey, U.K., 2003.
21. Cameron, R. J., "Advanced coupling matrix synthesis techniques for microwave filters," *IEEE Transactions on Microwave Theory and Techniques*, Vol. 51, No. 1, 1–10, Jan. 2003.
22. Cameron, R., "General coupling matrix synthesis methods for Chebyshev filtering functions," *IEEE Transactions on Microwave Theory and Techniques*, Vol. 47, No. 4, 433–442, Apr. 1999.
23. Kocbach, J. and K. Folgero, "Design procedure for waveguide filters with cross-couplings," *IEEE MTT-S Int Microwave Symp. Dig.*, Vol. 3, 1449–1452, Jun. 2002.
24. Huang, Q. and Z. Wu, "A compact six-order folded-waveguide resonator filter," *2018 IEEE MTT-S International Wireless Symposium (IWS)*, 2018.
25. Kojima, H., M. Nakahori, K. Matsutani, K. Kuroda, and K. Onaka, "A compact 28 GHz bandpass filter using quartz folded waveguide," *2018 IEEE MTT-S International Microwave Symposium (IMS)*, 2018.
26. Matsutani, K., et al., "Miniaturized quartz waveguide filter using double-folded structure," *2019 IEEE MTT-S International Microwave Symposium (IMS)*, 2019.